Biochemical and Biophysical Research Communications 443 (2014) 1162–1168

Contents lists available at ScienceDirect

Biochemical and Biophysical Research Communications

journal homepage: www.elsevier.com/locate/ybbrc

Ethyl pyruvate inhibits proliferation and induces apoptosis of hepatocellular carcinoma via regulation of the HMGB1–RAGE and AKT pathways

Ping Cheng [1], Weiqi Dai [1], Fan Wang, Jie Lu, Miao Shen, Kan Chen, Jingjing Li, Yan Zhang, Chengfen Wang, Jing Yang, Rong Zhu, Huawei Zhang, Yuanyuan Zheng, Chuan-Yong Guo *, Ling Xu *

Department of Gastroenterology, Shanghai Tenth People's Hospital, Tongji University of Medicine, Shanghai, People's Republic of China

ARTICLE INFO

Article history:
Received 5 December 2013
Available online 19 December 2013

Keywords:
Ethyl pyruvate
Hepatocellular carcinoma
Apoptosis

ABSTRACT

Ethyl pyruvate (EP) was recently identified as a stable lipophilic derivative of pyruvic acid with significant antineoplastic activities. The high mobility group box-B1 (HMGB1)–receptor for advanced glycation end-products (RAGE) and the protein kinase B (Akt) pathways play a crucial role in tumorigenesis and development of many malignant tumors. We tried to observe the effects of ethyl pyruvate on liver cancer growth and explored its effects in hepatocellular carcinoma model. In this study, three hepatocellular carcinoma cell lines were treated with ethyl pyruvate. An MTT colorimetric assay was used to assess the effects of EP on cell proliferation. Flow cytometry and TUNEL assays were used to analyze apoptosis. Real-time PCR, Western blotting and immunofluorescence demonstrated ethyl pyruvate reduced the HMGB1–RAGE and AKT pathways. The results of hepatoma orthotopic tumor model verified the antitumor effects of ethyl pyruvate in vivo. EP could induce apoptosis and slow the growth of liver cancer. Moreover, EP decreased the expression of HMGB1, RAGE, p-AKT and matrix metallopeptidase-9 (MMP9) and increased the Bax/Bcl-2 ratio. In conclusion, this study demonstrates that ethyl pyruvate induces apoptosis and cell-cycle arrest in G phase in hepatocellular carcinoma cells, plays a critical role in the treatment of cancer.

1. Introduction

Hepatocellular carcinoma (HCC) is the third most frequent cause of cancer-related death worldwide, and it has received considerable attention in recent years because of its increasing incidence [1,2]. Approximately 70% of these patients develop recurrent tumors within five years and rapidly progress to advanced stages, with a very low five-year survival rate of 7%. Therefore, there is an urgent need for new therapies to prolong the survival of patients with HCC.

Ethyl pyruvate (EP), a simple aliphatic ester derived from pyruvic acid, is more stable than pyruvic acid. It is a potent inhibitor of the inflammatory mediator late high mobility group box 1 (HMGB1) [3], and interferes with AKT pathways [4]. The HMGB1, the receptor for advanced generation end-products (RAGE), AKT pathways play crucial roles in tumorigenesis [5,6]. EP has been reported to induce apoptosis in many tumors, including gallbladder cancer, lung adenocarcinoma, and gastric cancer, yet its effects on HCC remain unclear [4,7,8]. Here, we investigated whether EP exerts an antitumor effect on hepatic tumor.

2. Materials and methods

2.1. Materials

EP was purchased from Sigma Aldrich (St. Louis, MO, USA) and stored in the dark at 4 °C. The antibodies (Santa Cruz Biotechnology, CA, USA) used for immunoblotting and immunohistochemical staining were: anti-BCL2, anti-Bax, anti-HMGB1, anti-p-AKT, anti-AKT, anti-MMP9.

2.2. Culture of tumor cell lines

The HCC cell lines SMMC-7721, HepG2, and HCC-LM3 (Chinese Academy of Sciences Committee Type Culture Collection Cell Bank) were maintained in 25 cm^2 polystyrene flasks (Corning Costar

* Corresponding authors.
E-mail addresses: guochuanyong@hotmail.com (C.-Y. Guo), xuling606@sina.com (L. Xu).
[1] These authors contributed equally to this work.

0006-291X/$ - see front matter © 2013 Elsevier Inc. All rights reserved.
http://dx.doi.org/10.1016/j.bbrc.2013.12.064

Corporation, Oneonta, NY) with high-glucose Dulbecco's modified Eagle's medium (DMEM-h; Thermo, China), containing 10% fetal bovine serum (FBS; Hyclone, South America), and 1% penicillin–streptomycin (Mediatech) in a humidified incubator at 37 °C in 5% CO_2.

2.3. Cell proliferation and viability

The HCC cell lines were plated at a density of 2×10^4 cells/well in 96-well plates in 100 μl of medium per well, then treated with EP of 0 μM, 6 μM, 12 μM, 18 μM, 24 μM, 30 μM, 36 μM, 42 μM and 48 μM. Finally, cell viability was measured using an MTT assay (Peptide Institute Inc., Osaka, Japan) and a microplate reader at a wavelength of 490 nm. A calibration curve was constructed using the data obtained from wells that contained known numbers of viable cells.

2.4. Detection of apoptosis and cell-cycle analysis using flow cytometry

Cell apoptosis was assessed using FITC (BD Pharmingen, San Jose, CA, USA). A flow-cytometric analysis was performed on cancer cells that were in the early apoptosis (annexin V^+/PI^-) or late apoptosis/necrosis (annexin V^+/PI^+) phase. The cell cycle was analyzed by flow cytometry and the percentages of cells in the different phases were calculated using the ModFit LT software (Verity Software House) [9].

2.5. Terminal deoxynucleotidyl transferase dUTP nick end labeling (TUNEL) assays

Tumor tissues from the saline-treated group and the EP-treated groups were analyzed with TUNEL assays. Sections (3 μm) from formalin-fixed paraffin-embedded tumors were deparaffinized with xylene and dehydrated with ethanol. The slides were rinsed twice with PBS and treated with proteinase K (15 μg/ml in 10 mM Tris/HCl, pH 7.4–8.0) for 15 min at 37 °C. Endogenous peroxidases were blocked with 3% hydrogen peroxide in methanol at room temperature for 10 min. The tissue sections were then analyzed with an in situ Cell Death Detection Kit, POD (Roche, Germany), in accordance with the manufacturer's instructions. The reaction was visualized with fluorescence microscopy.

2.6. Reverse transcription-polymerase chain reaction (RT-PCR) and real-time PCR

An RNeasy Mini Kit (Qiagen) was used to extract RNA from cells. Contaminating DNA was removed by DNase I digestion. cDNA was transcribed with an RT reagent kit with 2000 ng of RNA (per 20 μl reaction) and an oligo (dT) primer. The cDNA was then used as the template in real-time PCR reactions to analyze the expression of BCL2, Bax, HMGB1, MMP9 and β-actin. The primers used in the PCR reactions are listed in Table 1. The PCR reactions were performed with 10 min at 95 °C (hold), 40 cycles of amplification, each consisting of denaturation for 15 s at 95 °C, annealing for 1 min at 60 °C, and polymerization for 2 min at 72 °C in a 7900HT Fast Real-Time PCR System (ABI, Palo Alto, CA, USA). The relative mRNA levels were normalized to those of β-actin mRNA, and the fold change for each mRNA was calculated using the delta Ct method.

2.7. Western blot analysis

The total proteins were prepared with standard procedures and quantified by the BCA method. The sample proteins were separated by electrophoresis on SDS–polyacrylamide gel and transferred onto a polyvinylidene difluoride membrane. After blocking, the membranes were incubated overnight at 4 °C with various primary antibodies and β-actin. After incubation with peroxidase-conjugated secondary antibodies for 1 h at 25 °C, membranes were developed with the Odyssey Two-color Infrared Laser Imaging System (Li-Cor).

2.8. HCC model and treatment

Four-week-old male nude mice (athymic, BALB/C nu/nu) were purchased from Shanghai Slac Laboratory Animal Co., Ltd. All experiments were housed at the Experimental Animal Center, Tongji University at a constant temperature and with a consistent light cycle (light from 07:00 to 18:00). This study was carried out in strict accordance with the recommendations in the Guide for the National Science Council of the Republic of China. The protocol was approved by the Animal Care and Use Committee of The Tenth People's Hospital of Shanghai (Permit number: 2011-0111). This study was also approved by the Science and Technology Commission of Shanghai Municipality (ID: SYXK 2007-0006).

HCC-LM3 cells were suspended in 100 ml of 1:1 serum-free DMEM and Matrigel (BD Biosciences). One nude mouse was anesthetized with ketamine/xylazine, and HCC LM3 cells were seeded into the subcutaneous tissues and formed a subcutaneous tumor two weeks later. Then 30 nude mice were anesthetized with ketamine/xylazine, and their abdomens surgically opened. Tumor cells were inoculated subcutaneously into the liver parenchyma of the 30 nude mice and the mice were monitored every three days for 30 days. The 30 mice were then randomly allocated to one of three groups. Two groups were injected intraperitoneally with EP (40 mg/kg or 80 mg/kg) daily for four weeks and the control group was injected with saline on the same schedule. The mice were then killed and the tumors were measured with calipers.

2.9. Immunohistochemistry

Tumor tissues from saline-treated groups and EP-treated groups were used for immunohistochemistry. Sections (3 μm thick) from paraffin-embedded tumors were dewaxed with xylene, dehydrated with ethanol, and soaked in 3% hydrogen peroxide solution for 10 min to block endogenous peroxidase activity. The sections were boiled for 30 min in 10 mM citrate buffer (pH 6. 0) for antigen retrieval. The slides were incubated for 45 min with 5% BSA and incubated overnight at 4 °C with anti-HMGB1, MMP9 and anti-p-AKT antibodies. These specimens were incubated with the appropriate peroxidase-conjugated secondary antibody for

Table 1
Real-time PCR primer sequences.

Gene		Primer sequence (5′→3′)	Gene		Primer sequence (5′→3′)
Bcl-2	Forward	CATGTGTGTGGAGAGCGTCAA	Bax	Forward	GATCCAGGATCGAGCAGA
	Reverse	GCCGGTTCAGGTACTCAGTCA		Reverse	AAGTAGAAGAGGGCAACCAC
MMP-9	Forward	CGTCGTGATCCCCACTTACTATGGAAACTC	β-Actin	Forward	CTGGAACGGTGAAGGTGACA
	Reverse	GCAGAAGCCATACAGTTTATCCTGGTCATA		Reverse	AAGGGACTTCCTGTAACAATGCA
HMGB1	Forward	CGGATGCTTCTGTCAACTTCT	RAGE	Forward	CGGCTGGTGTTCCCAATAA
	Reverse	AGTTTCTTCGCAACATCACCA		Reverse	TGTTCCTTCACAGATACTCCCT

45 min at 37 °C and visualized with the Real Envision Detection Kit (Gene Tech Shanghai Company Limited, China), in accordance with the manufacturer's instructions. All slides were counterstained with hematoxylin and eosin (HE).

2.10. Immunofluorescence

The HCC cell lines were plated in 12-well plates and treated with EP (IC_{50}) for two days. The cells were washed three times with PBS for 1 min. The cells were fixed in 4% paraformaldehyde for 10 min on ice and then washed three times on ice with PBS for 3 min each. The cell membranes were ruptured with 0.2% Triton at room temperature for 20 min, and nonspecific antigen-binding sites were blocked by 5% BSA for 30 min. The cells were then incubated overnight at 4 °C with anti-HMGB1, and anti-MMP9 antibodies. On day 2, the nuclei were stained with DAPI (1:1000) after incubation with anti-rabbit antibody for 60 min. All cells were observed with a fluorescence microscope.

2.11. Statistical analyses

Statistical significance was assessed using the Student's *t*-test or ANOVA when appropriate using SPSS 16.0 (SPSS, Inc., Chicago, IL, USA). A $p < 0.05$ was considered significant.

3. Results

3.1. Ethyl pyruvate inhibits HCC in vitro and in vivo

The HCC cell lines (SMMC-7721, HepG2, and HCC-LM3) were treated with increasing concentrations of EP in an MTT assay. We constructed a growth curve to show the cytotoxicity of EP. With increasing concentrations of EP and time, EP caused a dose-dependent reduction in HCC cell viability in vitro; after 24 h, 48 h, and 72 h, the cell survival rates in the treated groups were lower than those in the corresponding control groups. These data indicate that EP reduces the viability of HCC cells in a significantly dose- and

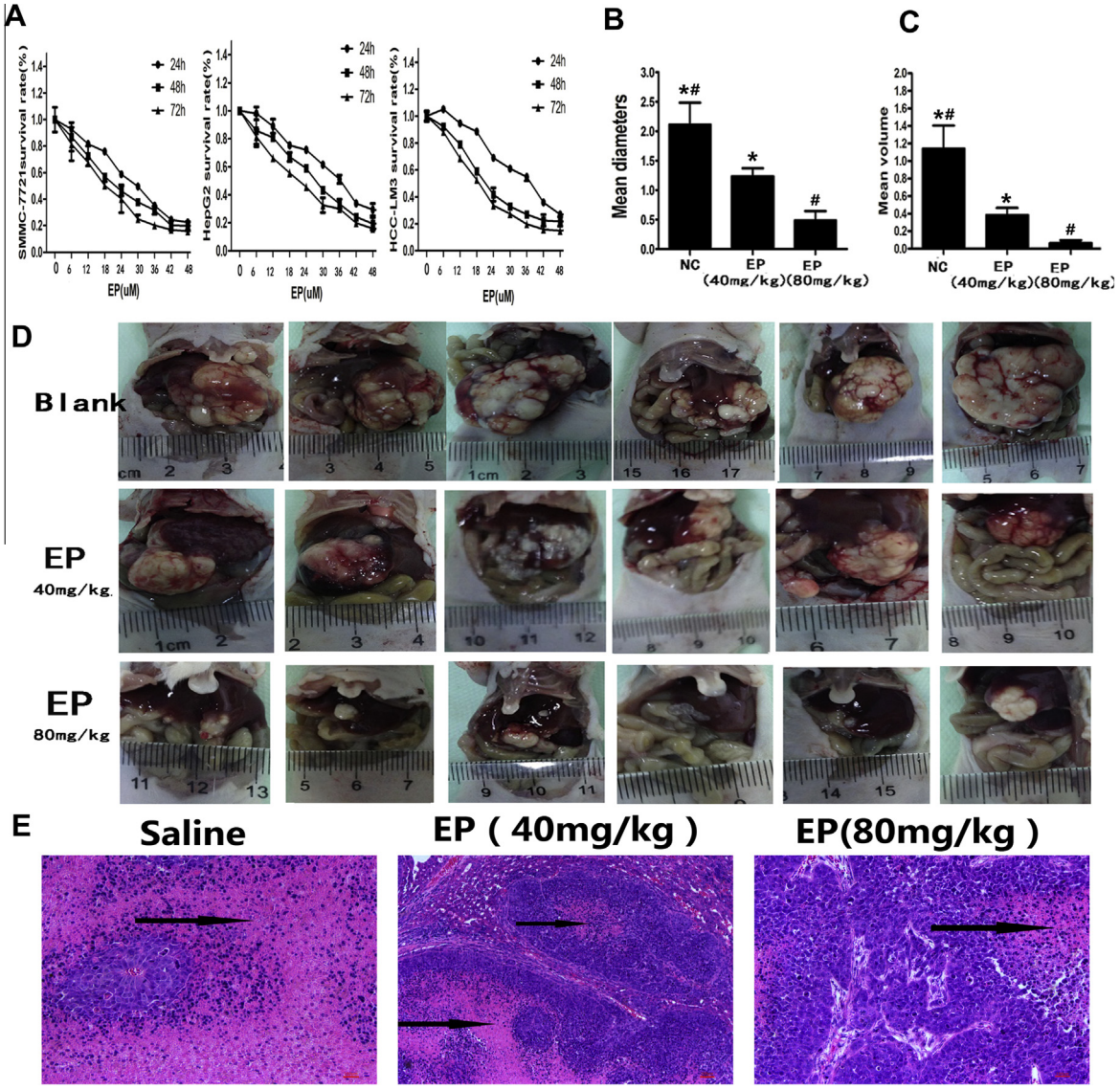

Fig. 1. EP inhibits HCC cell proliferation. (A) Cell viability was determined using a MTT assay. After 24 h, 48 h, and 72 h, the cell survival rates in the treated groups were lower than those in the corresponding control groups. (B) Tendency of tumor mean diameter after injection in nude mice (*$p < 0.05$). (C) Tendency of tumor mean volume after injection in nude mice (*$p < 0.05$). (D) Gross observation of HCC-LM3 cell orthotopic tumors in nude mice from the saline group or EP groups (40 mg/kg or 80 mg/kg). (E) Representative hematoxylin and eosin (H&E)-stained sections of liver showed the structure of the liver cancer tissue: nuclei of different sizes, hepatic cord structure was destroyed, magnification 200×.

time-dependent manner (Fig. 1A). Based on the results of MTT, we applied the concentration of SMMC-7721 (24.7 μM), HepG2 (29.7 μM), and HCC-LM3 (20.4 μM) for 48 h in the following experiments. To investigate the antitumor activities of EP in vivo, we established an HCC-LM3 model of in situ tumors in nude mice. After the administration of 40 mg/kg ethyl pyruvate, 80 mg/kg EP, or 10 g/μl saline for four weeks, the mice were killed. The liver tumors in the EP-treated groups were smaller than those in the control group (Fig. 1D). The mean diameter of the tumors decreased from 2.16 cm to 0.51 cm ($^*p < 0.05$; Fig. 1B) and the mean volume (V = length × width × 0. 5) of the tumors decreased from 1.187 cm^3 to 0.08945 cm^3 ($^*p < 0.05$; Fig. 1C). HE further confirmed the antitumor activities of ethyl pyruvate in vivo (Fig. 1E).

3.2. Ethyl pyruvate causes cell-cycle arrest and induces apoptosis

In this study, we found that ethyl pyruvate can inhibit the proliferation of HCC cell lines. Therefore, we investigated the mechanism of this inhibition. The effect of EP on the cell cycle was tested with a flow-cytometric analysis. As shown in Fig. 2A ($^*p < 0.05$), treatment with 29.7 μM EP for 48 h caused G2/M cell-cycle arrest in HepG2 cells, whereas 24.7 μM and 20.4 μM EP for 48 h induced G0/G1 phase arrest in SMMC-7721 and HCC-LM3 cells, respectively. Our results indicate that EP triggers cell-phase arrest differently in different HCC cells. We used flow cytometry to examine whether EP induces apoptosis. An increase in the percentages of cells in early apoptosis (quadrant 2) plus late apoptosis (quadrant 3) was identified in the HCC cell lines after treatment with ethyl pyruvate (Fig. 2B). Real-time PCR and Western blotting revealed that ethyl pyruvate treatment increased the BAX/BCL2 ratio in the HCC cell lines (Fig. 2C and D; $^*p < 0.05$). In vivo, TUNEL staining, Real-time PCR, Western blotting and Immunohistochemistry also demonstrated an increase in tumor cell apoptosis after treated with EP (Fig. 4; $^*p < 0.05$).

3.3. Ethyl pyruvate inhibits the HMGB1–RAGE and AKT pathways

To further clarify the mechanism underlying the effect of EP on HCC cells, we measured the inhibition of HMGB1 and AKT expression in HCC cells treated with EP using real-time PCR, Western blotting, and immunofluorescence analyses. The results showed that EP-treatment significantly reduce the c-DNA expression of HMGB1, RAGE and MMP9 (Fig. 3A, $^*p < 0.05$). With Western blotting and immunohistochemistry showed the expression of HMGB1, RAGE, p-AKT and MMP9 were significantly downregulated compared with those in the controls (Fig. 3B, $^*p < 0.05$). Finally, we evaluated the expression of HMGB1 and MMP9 with immunofluorescence (Fig. 3C, $^*p < 0.05$) and verified that EP downregulates the expression of HMGB1, and MMP9 in HCC. In vivo, the results of Real-time PCR, Western blotting and Immunohistochemistry also verified that EP could inhibit the HMGB1–RAGE and AKT pathways.

4. Discussion

HCC is the third most frequent cause of cancer-related death worldwide, and its incidence is increasing. Because there are no obvious symptoms in the early stages of HCC [10], many patients are diagnosed too late for surgery, so chemotherapy is still one of the most important treatments for liver cancer. Ethyl pyruvate (EP) is a commonly used food additive that is relatively nontoxic and harmless to the body [11]. It has been reported that EP can reduce the malignant traits of several types of cancer cells. For instance, EP inhibits gastric cancer growth by regulating the HMGB1–RAGE and AKT pathways [4]. EP inhibits the growth of colorectal tumors in the liver via induction of apoptosis [12]. In this study, we also found that EP exerts an anti-hepatoma effect by inhibiting the proliferation and inducing apoptosis (Figs. 1 and 2, $^*p < 0.05$). An MTT assay showed that the proliferation of HCC cell lines were inhibited after EP-treatment for 48 h (Fig. 1A). Flow

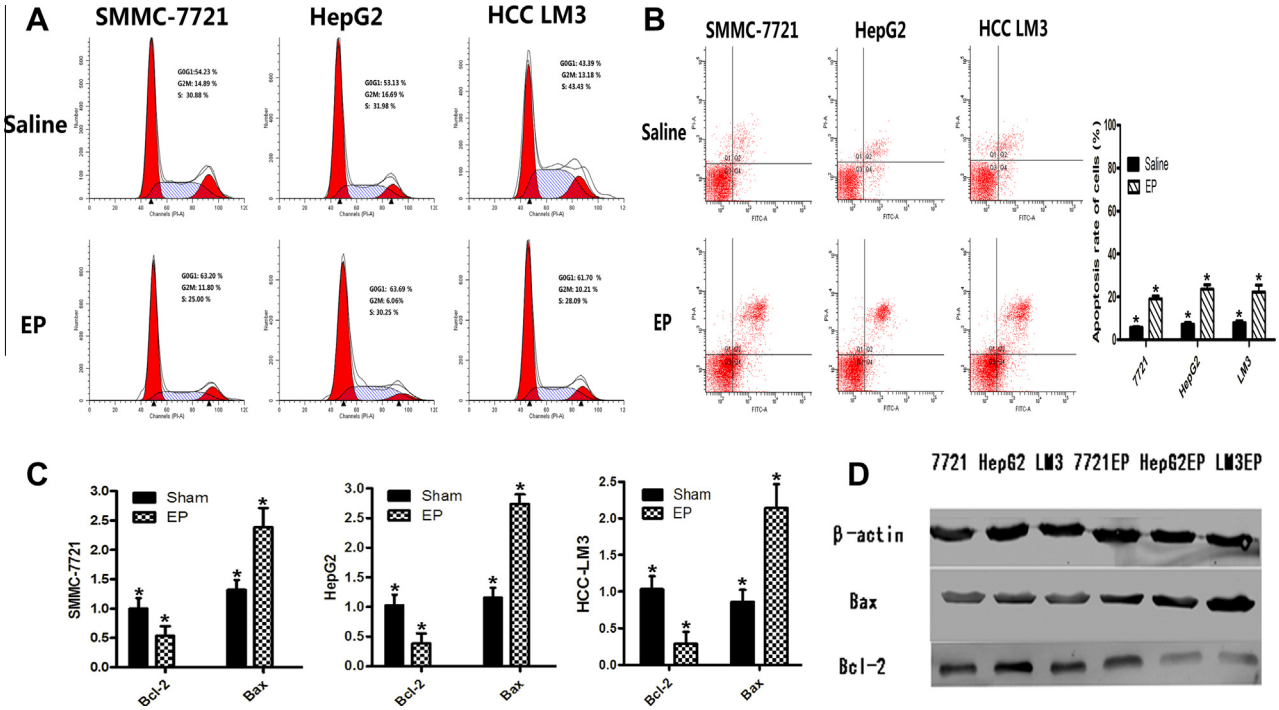

Fig. 2. EP causes cell cycle arrest and induces apoptosis in vitro. (A) EP causes cell cycle arrest of different HCC cells in different phases of the cell cycle. (B) EP induces apoptosis of HCC cells in vitro. Flow cytometric analyses of annexin-V/PI staining of SMMC-7721, HepG2 and HCC-LM3 cells. An increase in the percentages of cells in early apoptosis (quadrant 2) plus late apoptosis (quadrant 3) was identified in the HCC cell lines after treatment with EP ($^*p < 0.05$). (C) The expression of Bcl-2 and Bax on cDNA level was detected by real time PCR in vitro ($^*p < 0.05$ for Sham vs EP). (D) The expression of Bcl-2 and Bax on protein level was detected by Western blot in vitro.

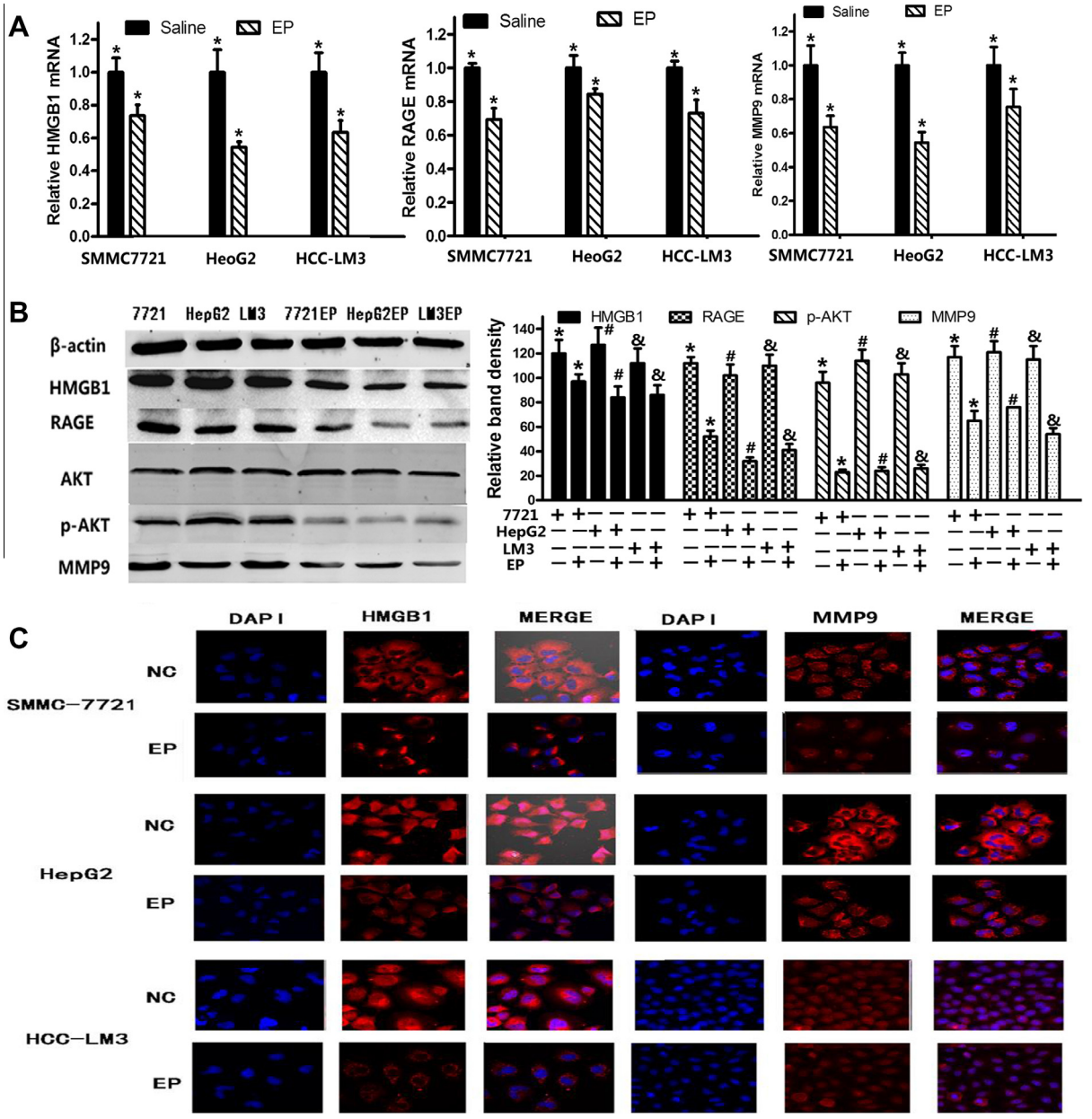

Fig. 3. EP inhibits HMGB, AKT signaling pathways in vitro. (A) The expression of HMGB1, RAGE, MMP9 in vitro on cDNA level was detected by real time PCR ($^{*}p < 0.05$ for Saline vs Saline + EP). (B) The expression of HMGB1, RAGE, p-AKT, MMP9 in vitro on protein level was detected by Western blot ($^{*}p < 0.05$ for Saline vs Saline + EP in SMMC-7721, $^{\#}p < 0.05$ for Saline vs Saline + EP in HepG2, & $p < 0.05$ for Saline vs Saline + EP in HCC-LM3). (C) The expression of HMGB1, MMP9 in vitro of different cell lines were shown by immunofluorescence (Original magnifications: ×400).

cytometry revealed the EP induced cell apoptosis and cell-cycle arrest in HCC cell lines after treatment for 48 h (Fig. 2A). The percentage apoptosis in the treatment groups was significantly greater than control groups ($^{*}p < 0.05$; Fig. 2B). In vivo, hepatocellular carcinoma model, HE and TUNEL assays also confirmed the ideas above (Figs. 1 and 4A, $^{*}p < 0.05$).

Moreover, the molecular mechanism of EP on hepatocellular carcinoma growth need be further explored. The HMGB1–RAGE and the AKT pathways are closely asso ciated with tumorigenesis of many cancers, such as HCC, gastrointestinal adenoma, colorectal cancer [13–15]. Recent studies have shown that the level of HMGB1 expression is consistent with the clinical cancer stage, which suggests that HMGB1 may be a tumor marker in HCC and that HMGB1-gene-targeted therapies may produce satisfactory outcomes [16]. RAGE as a membrane receptor expressed by a variety of cell types, it is overexpressed in many tumors and tumor-associated cells [17,18]. It's known that blockade of HMGB1–RAGE signaling pathways could result in attenuation of gastric cancer development and growth [4]. In addition, aberrant loss or gain of AKT activation underlies the pathophysiological prop erties of tumor growth and proliferation [19]. AKT and p-AKT have recently been shown to be highly expressed in liver carcinomas, and their expression may help predict the clinical outcome of liver cancer patients. [20] In our study, the results of Real-time PCR, Western blotting and immunohistochemical all show that EP could regulate of the HMGB1–RAGE and AKT pathways in HCC (Figs. 3 and 4).

Studies have demonstrated that AKT-induced MMP9 expression correlates strongly with HMGB1 expression [21]. Thieringer FR established a novel MMP9 transgenic mouse model, and report on a significantly increased susceptibility of MMP9 transgenic mice to chemically induced carcinogenesis [22]. Furthermore, it is

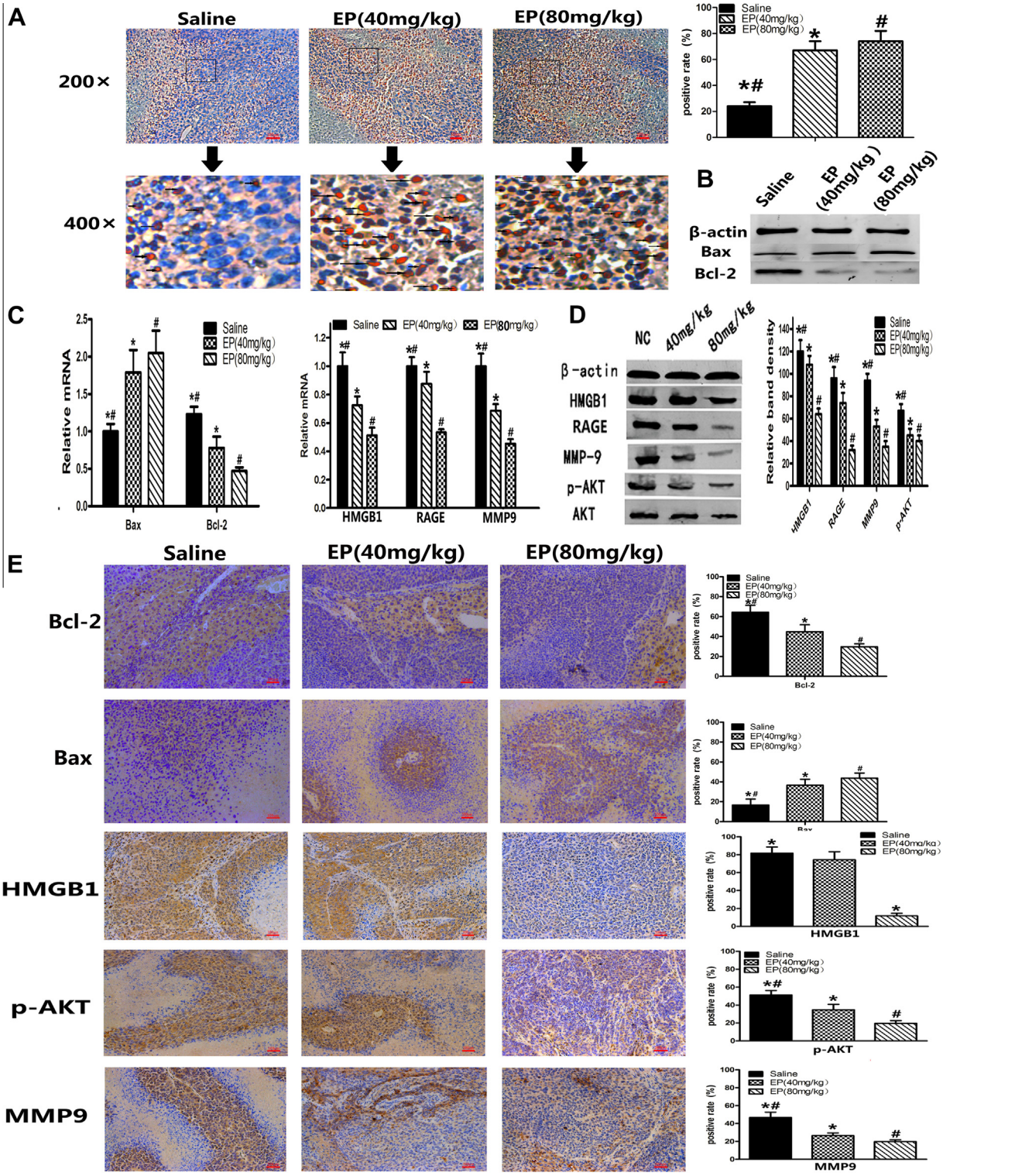

Fig. 4. The effects of EP in vivo. (A) TUNNEL staining showed the apoptotic cells in three groups at 8 h. Magnification 200× or 400× (*$p < 0.05$ for Saline vs Saline + EP (40 mg/kg), #$p < 0.05$ for Saline vs Saline + EP (80 mg/kg)). (B) The expression of Bcl-2 and Bax on protein level was detected by Western blot in vivo. (C) The expression of Bcl-2, Bax, HMGB1, RAGE, MMP9 on cDNA level was detected by real time PCR (*$p < 0.05$ for Saline vs Saline + EP (40 mg/kg), #$p < 0.05$ for Saline vs Saline + EP (80 mg/kg). (D) HMGB1, RAGE, p-AKT, MMP9 expression in vivo were evaluated by Western blot (*$p < 0.05$ for Saline vs Saline + EP (40 mg/kg), #p < 0.05 for Saline vs Saline + EP (80 mg/kg)). (E) The expression of Bcl-2, Bax, HMGB1, p-AKT, MMP9 in liver tissue of different groups was shown by immunohistochemistry (Original magnifications: ×200) (*$p < 0.05$ for Saline vs Saline + EP (40 mg/kg), #$p < 0.05$ for Saline vs Saline + EP (80 mg/kg)).

known that suppression of MMP9 could reduce tumor growth and induce apoptosis [23], we attempts to discover whether EP influences MMP9 expression. Our results verify that EP downregulates MMP9 expression in HCC cell lines (Figs. 3 and 4, *$p < 0.05$). Experimental results have suggested that HMGB1 combines with its ligand RAGE and activates MMP9, promoting tumor growth [4,24]. Other studies have demonstrated that HMGB1 attaches to key points on MMP9, increasing the generation of MMP9 protein

and improving gene activity to enhance exogenous tumor growth [25,26]. Therefore, EP reduces HMGB1 and MMP9 expression may have potential applications in liver cancer therapies.

It is well known that Bax promotes intrinsic apoptosis by forming oligomers in the mitochondrial outer membrane, participating in the release of apoptogenic molecules, oppositely, Bcl-2 inhibits mitochondrial apoptpsis by blocking the release and oligomerization of Bax. Our results showed that the balance between Bax and Bcl-2 trended to abnormal, with the increase of Bax and decrease of Bcl-2 with EP treatment (Fig. 2C and D, Fig. 4B, C and E, $^{*}p < 0.05$). In addition, the number of TUNEL-positive HCC cells and early apoptosis (quadrant 2) plus late apoptosis (quadrant 3) of flow cytometric analyses results had a significant increase, Hence, we supposed that EP ameliorated liver cancer by promoting the intrinsic pathway of apoptosis via positive regulation of the BAX/BCL2 ratio. Dai [27] report that TMZ/PYR inhibited the growth and induced cell cycle arrest, apoptosis of malignant tumors via negative regulation of MMP9 and positive regulation of the BAX/BCL2 ratio. In our study, Real time-PCR and Western blotting showed that EP down regulation the expression of the MMP9 proteins. Immunofluorescence and immunohistochemical confirmed these results (Figs. 3 and 4, $^{*}p < 0.05$). So we confidently conjecture that EP significantly inhibits the growth of liver cancer cells, and promotes tumor apoptosis via positive regulation of the BAX/BCL2 ratio, which might be mediated by the HMGB1–RAGE and AKT pathways.

In summary, EP, as a HMGB1 inhibitor, displayed marked anti-tumor proper ties and inhibited liver cancer growth, promotes apoptosis via positive regulation of the BAX/BCL2 ratio, which might be mediated by the HMGB1–RAGE and AKT pathways. It therefore constitutes a potential therapeutic agent for this aggressive malignancy.

Conflict of interest

All the authors have declared that no competing interests exist.

Acknowledgment

This work was supported by the National Natural Science Foundation of China (No. 81270515). The funder had no role in study design, data collection and analysis, decision to publish, or preparation of the paper.

References

[1] V. De Giorgi, L. Buonaguro, A. Worschech, et al., Molecular signatures associated with HCV-induced hepatocellular carcinoma and liver metastasis, PLoS One 8 (2013) e56153.
[2] A.M. Gerardi, L.P. Stoppino, A. Liso, et al., Rapid long-lasting biochemical and radiological response to sorafenib in a case of advanced hepatocellular carcinoma, Oncol. Lett. 5 (2013) 975–977.
[3] C. Lei, S. Lin, C. Zhang, et al., High-mobility group box1 protein promotes neuroinflammation after intracerebral hemorrhage in rats, Neuroscience 228 (2013) 190–199.
[4] J. Zhang, J.S. Zhu, Z. Zhou, et al., Inhibitory effects of ethyl pyruvate administration on human gastric cancer growth via regulation of the HMGB1–RAGE and Akt pathways in vitro and in vivo, Oncol. Rep. 27 (2012) 1511–1519.
[5] R. Kang, D. Tang, N.E. Schapiro, et al., The HMGB1/RAGE inflammatory pathway promotes pancreatic tumor growth by regulating mitochondrial bioenergetics, Oncogene (2013), http://dx.doi.org/10.1038/onc.2012.631.
[6] W. Wen, T. Han, C. Chen, et al., Cyclin G1 expands liver tumor-initiating cells by Sox2 induction via Akt/mTOR signaling, Mol. Cancer Ther. 12 (2013) 1796–1804.
[7] M.L. Li, X.F. Wang, Z.J. Tan, et al., Ethyl pyruvate administration suppresses growth and invasion of gallbladder cancer cells via downregulation of HMGB1–RAGE axis, Int. J. Immunopathol. Pharmacol. 25 (2012) 955–965.
[8] S.Y. Park, E.Y. Yi, M. Jung, et al., Ethyl pyruvate, an anti-inflammatory agent, inhibits tumor angiogenesis through inhibition of the NF-kappaB signaling pathway, Cancer Lett. 303 (2011) 150–154.
[9] F. Wang, L. He, W.Q. Dai, et al., Salinomycin inhibits proliferation and induces apoptosis of human hepatocellular carcinoma cells in vitro and in vivo, PLoS One 7 (2012) e50638.
[10] L. Jie, W. Fan, D. Weiqi, et al., The hippo-yes association protein pathway in liver cancer, Gastroenterol. Res. Pract. 2013 (2013) 187070.
[11] V.L. Cook, S.J. Holcombe, J.C. Gandy, et al., Ethyl pyruvate decreases proinflammatory gene expression in lipopolysaccharide-stimulated equine monocytes, Vet. Immunol. Immunopathol. 141 (2011) 92–99.
[12] X. Liang, A.R. Chavez, N.E. Schapiro, et al., Ethyl pyruvate administration inhibits hepatic tumor growth, J. Leukoc. Biol. 86 (2009) 599–607.
[13] H. Gao, H. Wang, J. Peng, Hispidulin induces apoptosis through mitochondrial dysfunction and inhibition of P13k/Akt signalling pathway in HepG2 cancer cells, Cell Biochem. Biophys. (2013).
[14] Y.N. Fahmueller, D. Nagel, R.T. Hoffmann, et al., Immunogenic cell death biomarkers HMGB1, RAGE, and DNAse indicate response to radioembolization therapy and prognosis in colorectal cancer patients, Int. J. Cancer 132 (2013) 2349–2358.
[15] W. Dai, F. Wang, L. He, et al., Genistein inhibits hepatocellular carcinoma cell migration by reversing the epithelial-mesenchymal transition: Partial mediation by the transcription factor NFAT, Mol. Carcinog. (2013), http://dx.doi.org/10.1002/mc.22100.
[16] N. Kohles, D. Nagel, D. Jungst, et al., Predictive value of immunogenic cell death biomarkers HMGB1, sRAGE, and DNase in liver cancer patients receiving transarterial chemoembolization therapy, Tumour Biol. 33 (2012) 2401–2409.
[17] T. Brenner, T.H. Fleming, D. Spranz, et al., Reactive metabolites and AGE-RAGE-mediated inflammation in patients following liver transplantation, Mediators Inflamm. 2013 (2013) 501430.
[18] M. Takada, K. Hirata, T. Ajiki, et al., Expression of receptor for advanced glycation end products (RAGE) and MMP-9 in human pancreatic cancer cells, Hepatogastroenterology 51 (2004) 928–930.
[19] S. Suman, V. Kurisetty, T.P. Das, et al., Activation of AKT signaling promotes epithelial-mesenchymal transition and tumor growth in colorectal cancer cells, Mol. Carcinog. (2013), http://dx.doi.org/10.1002/mc.22076.
[20] W. Jiang, Z. Zhu, H.J. Thompson, Dietary energy restriction modulates the activity of AMP-activated protein kinase, Akt, and mammalian target of rapamycin in mammary carcinomas, mammary gland, and liver, Cancer Res. 68 (2008) 5492–5499.
[21] K. Lolmede, L. Campana, M. Vezzoli, et al., Inflammatory and alternatively activated human macrophages attract vessel-associated stem cells, relying on separate HMGB1- and MMP-9-dependent pathways, J. Leukoc. Biol. 85 (2009) 779–787.
[22] F.R. Thieringer, T. Maass, B. Anthon, et al., Liver-specific overexpression of matrix metalloproteinase 9 (MMP-9) in transgenic mice accelerates development of hepatocellular carcinoma, Mol. Carcinog. 51 (2012) 439–448.
[23] Z. Li, X. Xu, L. Bai, et al., Epidermal growth factor receptor-mediated tissue transglutaminase overexpression couples acquired tumor necrosis factor-related apoptosis-inducing ligand resistance and migration through c-FLIP and MMP-9 proteins in lung cancer cells, J. Biol. Chem. 286 (2011) 21164–21172.
[24] S.J. Cho, M.J. Chae, B.K. Shin, et al., Akt- and MAPK-mediated activation and secretion of MMP-9 into stroma in breast cancer cells upon heregulin treatment, Mol. Med. Rep. 1 (2008) 83–88.
[25] R. Kang, D. Tang, N.E. Schapiro, et al., The receptor for advanced glycation end products (RAGE) sustains autophagy and limits apoptosis, promoting pancreatic tumor cell survival, Cell Death Differ. 17 (2010) 666–676.
[26] T. Sasahira, T. Kirita, N. Oue, et al., High mobility group box-1-inducible melanoma inhibitory activity is associated with nodal metastasis and lymphangiogenesis in oral squamous cell carcinoma, Cancer Sci. 99 (2008) 1806–1812.
[27] C. Dai, B. Zhang, X. Liu, et al., Pyrimethamine sensitizes pituitary adenomas cells to temozolomide through cathepsin B-dependent and caspase-dependent apoptotic pathways, Int. J. Cancer 133 (2013) 1982–1993.